Tunable terahertz Bloch oscillations in chirped photonic crystals

Virginie Lousse[1,2,*] and Shanhui Fan[2]
[1]*Laboratoire de Physique du Solide, Facultés Universitaires Notre-Dame de la Paix, B-5000 Namur, Belgium*
[2]*Ginzton Laboratory, Stanford University, Stanford, California 94305, USA*
(Received 22 April 2005; published 12 August 2005)

We report simulations showing tunable terahertz oscillations of the electromagnetic field provided by the Bloch oscillations of a short photonic wave packet in a tilted band structure. The structure consists in a finite one-dimensional photonic crystal inhomogeneously chirped by a slowly-varying refractive index gradient. Tunability is obtained by relocating the Bloch oscillations center in regions characterized by different local band structure gradients. With reasonable refractive indexes, this mechanism may allow the generation of signals which cover a wide continuous part of the electromagnetic terahertz range, when used in combination of appropriate detection schemes.

DOI: 10.1103/PhysRevB.72.075119 PACS number(s): 42.70.Qs, 78.67.Pt, 71.20.−b, 42.65.Re

I. INTRODUCTION

Terahertz radiations, sometimes referred to as *T-rays*, belong to a particularly useful part of the electromagnetic spectrum. Much of the interest for this electromagnetic spectral range stems from the ability of this radiation to penetrate deep into biological tissue, with the advantage over x-rays that it does so without inducing ionization damages. Terahertz wavelengths extend from 30 μm (10×10^{12} Hz) to 1 mm (0.3×10^{12} Hz), i.e., those frequencies which bridge microwaves to infrared light. For physical reasons, absorption and reflection of matter in this spectral range are usually found to be quite different from the corresponding properties in the other parts of the spectrum. Exploitations of these peculiar characteristics have been considered in many fields, such as biomedical sensing,[1] radioastronomy,[2] studies of the Earth atmosphere,[3] plasma fusion diagnostics,[4] and gas spectroscopy.[5] Practical methodologies using these radiations have been developed for security monitoring.[6] In spite of limitations in imaging resolution, terahertz radiation is believed to provide a way to visually discriminate materials which often have the same appearance under visible-light illumination. The early detection of skin cancer, for instance, is one of the recent suggestions for application.[1]

The use of terahertz radiation has been boosted by the very recent development of efficient sources. Remarkably, Köhler *et al.*[7] introduced a semiconductor laser that produces intense radiation at 4.4 THz, by injecting carriers into a semiconductor quantum well. In parallel, synchrotron radiation can also be used,[8] producing incoherent radiation in a very wide spectral range. Many other approaches have been attempted, including direct laser-to-laser spectral conversions. For instance, optical mixing in nonlinear crystals[9,10] or in photoconductors,[11–14] quantum cascade lasing[15,16] or oscillation of semiconductor resonant tunneling diodes[17–19] are competing for reliably producing terahertz radiation. More references and techniques will be found in a recent review article by Peter H. Siegel.[20]

In the present work, we describe a mechanism which can be used for the tunable terahertz modulation of infrared radiation. The fundamental idea is to exploit the Bloch oscillations of photonic carriers, which have clearly been observed in one-dimensional photonic crystals.[21,22] With an appropriate detection process, this could lead to the generation of tunable radiation in the terahertz spectral range.

II. MOTIONLESS TUNABLE CAVITY USING BLOCH OSCILLATIONS

Bloch oscillations arise from an intraband process which has first been experimentally demonstrated in semiconductor superlattices in the presence of a uniform electric field.[23–25] Originally proposed for atomic crystals,[26–29] the phenomenon could not be observed there because competing interband transitions usually preclude the formation of a complete oscillation.[30] The photonic analogue of this effect appears when a photonic crystal is subject to a slowly varying refractive index or a geometry parameter modulation, resulting in a linear tilting of the band structure. These "chirped" photonic crystals give rise to a set of equidistant frequency levels, the optical counterpart of the Wannier-Stark ladder in semiconductor superlattices. The tilting of the photonic bands can be obtained in different ways. In confined Bragg mirrors, the band structure gradients are caused by a gradual change of the lateral confinement;[31] in graded-index optical superlattices, the gradient stems from a linear modification of the layers refractive indexes;[22] in geometrically chirped photonic crystals, the band structure modulation arises from a gradual modification of the layers thicknesses.[21] A theoretical description of the photonic Bloch oscillations for geometrically chirped photonic crystals can be found in a paper by Malpuech *et al.*[32]

Figure 1 shows the graded-index structure considered in this work. This photonic device can be described as a series of n cavities separated from each other and from the incidence and emergence media by Bragg mirrors made of multiple quarter-wave layers. The refractive index of the layers is set to vary in a non-uniform way, in order to control the local values of the Bloch oscillations frequencies along the film depth, perpendicular to the layers. Such a fine adjustment of the refractive indexes is possible in special cases, as with porous silicon, where changes in etching anodization current control the variations of the optical density.[33] If i is

 ©2005 The American Physical Society

FIG. 1. View of the structure considered in this paper. Wide cavities of equal thicknesses $d_{cav}=541$ nm are separated by distributed Bragg mirrors which assemble five layers of thicknesses $d_a=135$ nm (clear) and $d_b=100$ nm (dark). The whole structure contains n wide cavities (our calculations use $n=20$), and $n+1$ mirrors. The refractive index (increasing with darker gray shades) of these layers is not periodic, but gradually modified along the depth of the structure.

the cavity number, the refractive indexes in each period (containing one reflector and one cavity) are described by the values taken from the (backward) recurrence rule

$$n_i = \frac{n_{i+1}}{1 + \left[(g_2 - g_1)\frac{i-1}{n-1} - g_2 \right] \frac{d_{cav}}{hc} n_{i+1}}. \quad (1)$$

In these relations, g_1 and g_2 are parameters which approximate the limits of the targeted tunability range of the terahertz device, as a radiation emitter (values such as $g_1=1.5$ meV and $g_2=60$ meV are adequate to attempt covering the entire terahertz radiation range). In what follows, the number of cavities is set to $n=20$ and the cavity width d_{cav} is given the constant value 541 nm. The reflector layers are quarter-wave slabs, with respective indexes and thicknesses $n_a=1.45$ and $d_a=135$ nm, and $n_b=1.95$ and $d_b=100$ nm in the rear ($i=20$) period. The cavity index, in the rear period, is also $n_{cav}=n_a$. In previous works,[22] the target was to obtain a refractive index modulation which led to a nearly linear band tilting, providing only one Bloch oscillation frequency. Here we will require that, within the depth of the film, the band structure gradient spans a whole range of values, which will all be available to provide a range of terahertz oscillation frequencies. The above nonlinear recursion, Eq. (1), not only provides a slow spatial modulation of the refractive indexes but also a slow linear change of its gradient. The resulting photonic structure can be understood in terms of a local band structure gradient across the depth of the device, using concepts borrowed from the effective-mass theory of semiconductors. Figure 2 shows the actual band and gap regions as a parabolic depth-dependent (i.e., z-dependent) band structure. This calculation takes the parameters found in the chirped finite film at a given depth z, and evaluates the location of the gaps of an infinite photonic crystal defined by these parameters. This figure also shows the total reflectance of the sample, where the Wannier-ladder resonances are clearly observed. The spacing of this levels decreases for increasing energies, in relation with the band structure curvature. The amplitude of these dips varies according to the length of gap regions to be crossed by the transiting light. The absence of transmission between 1.3 and 1.4 eV is only related to the high reflection on the lowest gap. It should be emphasized that even in that case, light penetrates in the band between the two gaps, where it undergoes its Bloch oscillations.

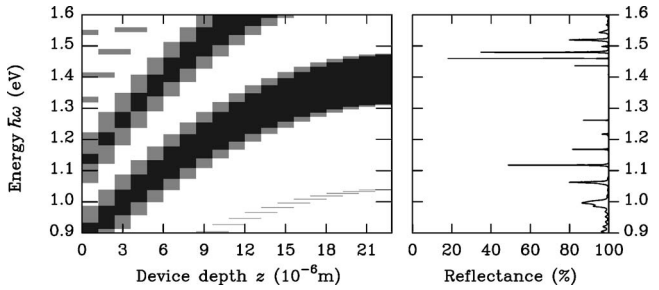

FIG. 2. Slow modification of the local band structure across the multilayer stack arising from the nonlinear modulation of refractive indexes. The black and gray areas correspond to local gaps, where no "normal-incidence" photonic states appear. Note that the slope of the band edges is not constant. The reflectance spectrum, on the right inset, reveals features related to Bloch oscillations and the Zener effect.

These resonances correspond to very high quality-factor states.

Figure 3 shows the square of the electric field inside the structure along the growth direction z for a range of frequencies matching that of the band structure in Fig. 2. In this representation, a monochromatic plane wave at normal incidence is assumed to inject energy in the multiple-scattering structure. The upper-left region of Fig. 3 shows the interference between the incident wave, entering the chirped photonic crystal and the back-running wave reflected on the higher gap. Undergoing Zener tunneling, some of the light crosses the gap elastically and feeds the horizontal resonances associated with the Wannier ladder, providing Bloch oscillations. These resonances appear inside the band which separates the higher and lower gaps shown on Fig. 2. The center of the band defines, in space, the center of the Bloch oscillations. Due to our choice of the structure parameters, the spacing of the levels on this Wannier ladder covers a large part of the terahertz electromagnetic range. The spectral location of

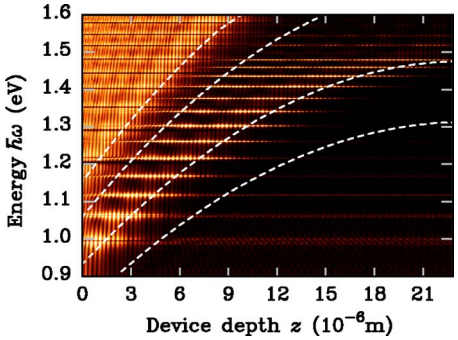

FIG. 3. (Color online) Square of the electric field $E(z,\omega)$ inside the structure (along the growth direction z), for a range of frequencies matching that of Fig. 2. The horizontal resonances are the Wannier-Stark ladder levels requested for intraband Bloch oscillations. These resonances appear inside the band confined between the local gaps, defined as in Fig. 2. When considering decreasing photon energies, a gradual increase of the level spacing is observed, together with a spatial shift of the Bloch oscillations center. This is due to the curvature introduced in the refractive index distribution described by Eq. (1).

these ladder levels exactly matches the series of dips observed on the reflectance spectrum of Fig. 2. A gradual change of spacing of the Wannier levels follows any incident photon frequency change, or Bloch oscillations center shift, due to the nonlinear modulation given to the refractive index of the layers.

Note that the distance between successive frequency levels can be obtained by the following Fabry-Perot formula:

$$\Delta(\bar{h}\omega) = \frac{hc}{2d\bar{n}}, \tag{2}$$

where d is the local distance between the gap edges at the given input frequency and $\bar{n}$ is the average refractive index. This estimate fits adequately the levels observed in Fig. 3, as a function of the film depth.

III. ADJUSTABLE OSCILLATING PATHS

A short pulse of infrared radiation injected in this chirped one-dimensional photonic crystal can be described as a Bloch wave packet characterized by an experimentally defined central frequency ω_0. The dynamics of this wave packet is ruled by the superposition principle. The wave-packet envelope evolves in time inside the structure as

$$E(z,t) = \frac{1}{2\pi}\int_{-\infty}^{+\infty} E(z,\omega)g(\omega)e^{-i\omega t}\,d\omega, \tag{3}$$

where $E(z,\omega)$ represents the field amplitude which develops in the layers under an incident monochromatic wave (see Fig. 3). $g(\omega)$ is the Fourier coefficient of the incident pulse. For a gaussian wave falling under normal incidence, this is essentially proportional to

$$g(\omega) \propto \exp\left[-\left(\frac{\omega-\omega_0}{\Delta\omega}\right)^2\right]. \tag{4}$$

The parameter $\Delta\omega$ controls the pulse duration, which should be sized to a value close to the Bloch oscillations periods (a typical 100 fs). The central frequency ω_0 is set at an order of magnitude in relation with the photonic crystal spectral response, typically in the eV range.

Figure 4 shows the wave-packet law of motion, in z-space and time, for different values of the incident pulse central frequency ω_0. Space oscillations are clearly seen in all cases, as expected, but the center and the frequency of the oscillations change with ω_0. In Fig. 4(a), the incident pulse frequency is $\hbar\omega_0=1.2$ eV and the oscillations period is found to be 85 fs (11.8 THz), compared to 84 fs (49 meV) read on the reflectance spectrum of Fig. 2; in Fig. 4(b), the incident pulse frequency is $\hbar\omega_0=1.3$ eV and the oscillations period is found to be 106 fs (9.4 THz), compared to 104 fs (40 meV) from reflectance; in Fig. 4(c), the incident pulse frequency is $\hbar\omega_0=1.45$ eV and the oscillations period is found to be 189 fs (5.3 THz), compared to 188 fs (22 meV). It is important to underline that the parameters used to define the initial photonic structure can be widely modified, leaving much room for further optimization of the Bloch oscillations generator.

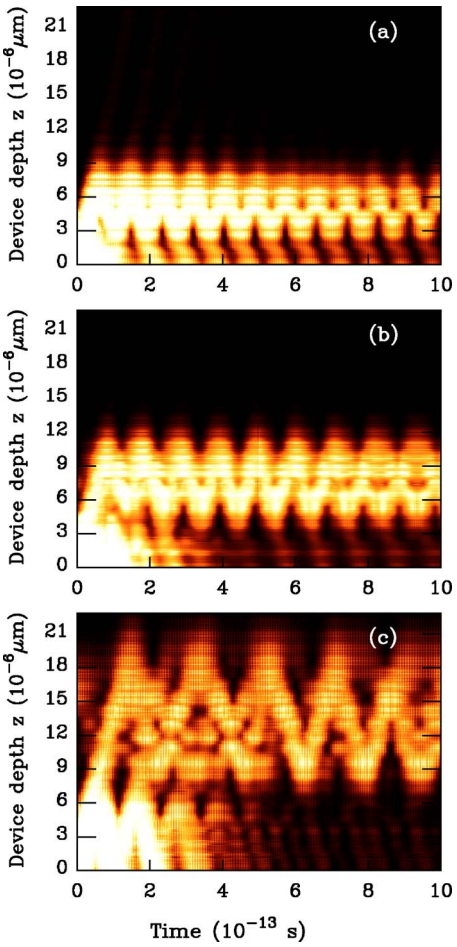

FIG. 4. (Color online) Spatial Bloch oscillations obtained when the chirped photonic crystal is hit by a short pulse of infrared radiation, for different values of the central wave-packet frequency ω_0. The different panels correspond to 100 fs Gaussian pulses with different incident carrier frequencies: (a) $\hbar\omega_0=1.2$ eV; (b) $\hbar\omega_0=1.3$ eV; (c) $\hbar\omega_0=1.45$ eV. The Bloch oscillations clearly develop around different centers, with different periods.

The above analysis provides a handle for Bloch oscillations tunability: The infrared pulse, when scattered by the structure undergoes oscillations at different depth in the device according to the incident central frequency. The shift of the oscillation center allows the wave-packet to start oscillating in regions of different refractive index gradients which leads to various Bloch oscillations frequencies. This phenomenon is clearly specific to Bloch oscillators: Fixed-boundary cavities (as in Fabry-Pérot devices), for instance, can produce oscillations of a spatially confined wave packet, but the center of oscillations cannot be changed, making it difficult to achieve tunability.

IV. DETECTION OF TERAHERTZ FIELDS

It remains to consider the extraction of the terahertz signal from the bouncing wave-packet. There are two distinct aspects to this question. First, the electromagnetic signal must escape from the oscillation path in the form of an infrared terahertz-modulated carrier wave. Second, some detection

system must extract the terahertz signal from the infrared modulated wave.

The first question involves the transfer of energy from the oscillating spatial range into the medium outside the film. During Bloch oscillations, the electromagnetic wave is periodically reflected on the gap boundaries. This reflection competes with the interband transmission through the bandgaps known as the Zener effect. This process consists in an elastic tunneling transition through a local gap and provides an opportunity for the energy to escape from the device. With a short pulse, this transmission and reflection is attempted at twice the Bloch oscillations frequency. The intensity of this escaping signal increases with the probability of a Zener process, depending on the gap lengths. In the examples provided by Fig. 4, the case $\hbar\omega_0=1.3$ eV [Fig. 4(b)] corresponds to the wider exiting gap. Because of the reduction of the Zener effect probability, the lifetime of the Bloch oscillations is maximal and the wave-packet field is maintained much longer than for the other injected frequencies. A longer-lasting emission then requires a low Zener tunneling probability and a high storage of energy in the wave-packet. This can be better achieved with wider gaps.

The detection of terahertz radiation, i.e., the suppression of the carrier frequency from the exiting modulated wave is the subject of ongoing studies.[34–38] Several directions have been pursued with results showing various efficiencies.

One direction is that of miniaturized whisker diodes, which was proposed by Cutler *et al.*[35] as a result of the analysis of the asymmetric response to electromagnetic fields of the scanning tunnelling microscope. The size reduction of the metal-tip diode to near-atomic scale moves the rectification capability from radio or microwaves to optical frequencies. These studies then suggest that, for the present purpose, the detection could be achieved in spatially distributed arrays of whiskers facing flat conductor surfaces.

Another direction is offered by the nonlinear wave mixing in which difference frequencies can easily be generated. The spectrum of a modulated infrared signal, as shown on Fig. 4, can actually be deduced from the spectrum of Fig. 3, at a specific depth in the device. The available frequencies are described by the recurrence relation

$$\omega_i = \omega_{i-1} + \Delta\omega_i \tag{5}$$

where $\Delta\omega_i$ is the difference frequency generated with an infrared incident beam of frequency close to ω_i. Lithium niobate was recently suggested as a possible material in which the required infrared-to-terahertz nonlinear conversion can be realized.[39]

V. CONCLUSION

Bloch oscillations and the Zener effect in photonic crystals are not just interesting analogues of the Bloch oscillations and the Zener effect of charge carriers in semiconductors. The use of chirped photonic crystals allows to define a new type of Fabry-Perot cavity, where the reflectors are replaced by non propagating regions associated with the local periodicity of the structure. The spatial location of the wave turning point, where the reflection occurs, change with the frequency of the incident wave. With a well-designed gradual modification of the structure, it is possible to modify the distance between the turning points by a mere adjustment of the incident frequency. We then obtain a very effective cavity tuning without any mechanical change of the cavity geometry and with no externally driven modification of the refractive index of the material.

In the present work, it is suggested to use this very peculiar cavity to produce a long-lasting infrared optical wave carrying a terahertz oscillating modulation. The idea is to inject a short, but energetic, pulse of infrared radiation into the chirped-crystal cavity and let it resonate by multiple reflection on the inner gaps, undergoing spatial Bloch oscillations. A careful choice of the spatial chirping of the structure will lead to frequency separations which can span a significant part of the terahertz spectral range. This can be used to produce a large number of distinct terahertz modulation frequencies, which can be tuned by adjusting the frequency of the incident infrared beam. In the simulations supporting this idea, we took care of keeping all material and geometry parameters within the range of availability. However, only the practical realization of the device will provide a real proof a feasibility.

The detection of the modulation is then essential for producing the final radiation. The technical details of this stage of the process have not been described, but it was realized that a nonlinear filter is required, either to rectify the modulated carrier, as with miniaturized whisker diodes arrays, or by difference frequency generation.

ACKNOWLEDGMENTS

V.L. was supported as Postdoctoral Fellow by the Belgian National Fund for Scientific Research (FNRS). The authors thank Professor Jean Pol Vigneron (University ND de la Paix, Namur, Belgium) for critically reading the manuscript and many suggestions.

*Electronic address: virginie.lousse@stanford.edu

[1] E. Pickwell, B. E. Cole, A. J. Fitzgerald, M. Pepper, and V. P. Wallace, Phys. Med. Biol. **49**, 1595 (2004).

[2] T. G. Phillips and J. Keene, Proc. IEEE **80**, 1662 (1992).

[3] J. W. Waters, Proc. IEEE **80**, 1679 (1992).

[4] N. C. Luhmann and W. A. Peebles, Rev. Sci. Instrum. **55**, 279 (1984).

[5] R. H. Jacobsen, D. M. Mittleman, and M. C. Nuss, Opt. Lett. **21**, 2011 (1996).

[6] D. Woolard, R. Kaul, R. Suenram, A. H. Walker, T. Globus, and A. Samuels, IEEE MTT-S Int. Microwave Symp. Dig. **3**, 925 (1999).

[7] R. Koehler, A. Tredicucci, F. Beltram, H. E. Beere, E. H. Linfield, A. G. Davies, D. A. Ritchie, R. C. Iotti, and F. Rossi, Nature (London) **417**, 156 (2002).
[8] M. Abo-Bakr, J. Feikes, K. Holldack, P. Kuske, W. B. Peatman, U. Schade, G. Wustefeld, and H.-W. Hubers, Phys. Rev. Lett. **90**, 094801 (2003).
[9] K. Kawase, M. Sato, T. Taniuchi, and H. Ito, J. Appl. Phys. **68**, 2483 (1996).
[10] X. Zernike and P. R. Berman, Phys. Rev. Lett. **15**, 999 (1965).
[11] E. R. Brown, F. W. Smith, and K. A. McIntosh, J. Appl. Phys. **73**, 1480 (1993).
[12] E. R. Brown, K. A. McIntosh, K. B. Nichols, and C. L. Dennis, Appl. Phys. Lett. **66**, 285 (1995).
[13] S. Matsuura, G. A. Blake, R. A. Wyss, J. C. Pearson, C. Kadow, A. W. Jackson, and A. C. Gossard, Appl. Phys. Lett. **74**, 2872 (1999).
[14] T. Noguchi, A. Ueda, H. Iwashita, S. Takano, T. Ishibashi, H. Ito, and T. Nagatsuma, Proceedings of the 12th Int. Space Terahertz. Technol. Symp., 2001, p. 3.2.
[15] J. H. Smet, C. F. Fonstad, and Q. Hu, J. Appl. Phys. **79**, 9305 (1996).
[16] B. Xu, Q. Hu, and M. R. Melloch, Appl. Phys. Lett. **71**, 440 (1997).
[17] E. R. Brown, J. R. S. C. D. Parker, J. Mahoney, K. M. Molvar, and T. G. McGill, Appl. Phys. Lett. **58**, 2291 (1991).
[18] T. C. L. G. Sollner, W. D. Goodhue, P. E. Tannenwald, C. D. Parker, and D. D. Peck, Appl. Phys. Lett. **43**, 588 (1993).
[19] M. Reddy, S. C. Martin, A. C. Molnar, R. E. Muller, R. P. Smith, P. H. Siegel, M. J. Mondry, M. J. Rodwell, and J. S. J. Allen, Proceedings of the 8th Int. Space Terahertz Technol. Symp., 1997, p. 149.
[20] P. H. Siegel, IEEE Trans. Microwave Theory Tech. **50**, 910 (2002).
[21] V. Agarwal, J. A. delRio, G. Malpuech, M. Zamfirescu, A. Kavokin, D. Coquillat, D. Scalbert, M. Vladimirova, and B. Gil, Phys. Rev. Lett. **92**, 097401 (2004).
[22] R. Sapienza, P. Costantino, D. Wiersma, M. Ghulinyan, C. J. Oton, and L. Pavesi, Phys. Rev. Lett. **91**, 263902 (2003).
[23] L. Esaki and R. Tsu, IBM J. Res. Dev. **14**, 61 (1970).
[24] C. Waschke, H. G. Roskos, R. Schwedler, K. Leo, H. Kurz, and K. Kohler, Phys. Rev. Lett. **70**, 3319 (1993).
[25] M. Kushwaha, Surf. Sci. Rep. **41**, 1 (2001).
[26] F. Bloch, Z. Phys. **52**, 555 (1928).
[27] C. Zener, Proc. R. Soc. London, Ser. A **145**, 523 (1934).
[28] H. James, Phys. Rev. **76**, 1611 (1949).
[29] G. Wannier, Phys. Rev. **100**, 1227 (1955).
[30] J. M. Ziman, *Principles of the Theory of Solids* (Cambridge University Press, Cambridge, 1972).
[31] A. Kavokin, G. Malpuech, A. DiCarlo, P. Lugli, and F. Rossi, Phys. Rev. B **61**, 4413 (2000).
[32] G. Malpuech, A. Kavokin, G. Panzarini, and A. DiCarlo, Phys. Rev. B **63**, 035108 (2001).
[33] V. Agarwal and J. A. del Rio, Appl. Phys. Lett. **82**, 1512 (2003).
[34] M. Bass, P. A. Franken, J. F. Ward, and G. Weinreich, Phys. Rev. Lett. **9**, 446 (1962).
[35] P. H. Cutler, T. E. Feuchtwang, T. T. Tsong, H. Nguyen, and A. A. Lucas, Phys. Rev. B **35**, 7774 (1987).
[36] S. L. Chuang, S. Schmitt-Rink, B. I. Greene, P. N. Saeta, and A. F. J. Levi, Phys. Rev. Lett. **68**, 102 (1992).
[37] C. Bosshard, R. Spreiter, M. Zgonik, and P. Gunter, Phys. Rev. Lett. **74**, 2816 (1995).
[38] Y.-S. Lee, T. Meade, V. Perlin, H. Winful, T. B. Norris, and A. Galvanauskas, Appl. Phys. Lett. **76**, 2505 (2000).
[39] C. Weiss, G. Torosyan, J.-P. Meyn, R. Wallenstein, and Y. H. Avetisyan, Opt. Express **8**, 497 (2001).